

Comfortable Body Surface Potential Mapping by Means of a Dry Electrode Belt

Roman Kusche¹, Andra Oltmann¹, Jan Graßhoff¹, and Philipp Rostalski¹

Abstract—Body Surface Potential Mapping is the spatial high-resolution acquisition of cardiac electrical activity from the thorax surface. The method is used to record more comprehensive cardiac information than conventional ECG measurement approaches. Although Body Surface Potential Mapping is well-known and is technically feasible, it is rarely used in clinical environments. One reason for this is the cumbersome procedure of a measurement. The placement of many adhesive gel electrodes and the contacting with many cables are particularly problematic. These limit both patients and medical staff. Therefore, the goal of this work is to technically simplify Body Surface Potential Mapping so that it would be applicable under clinical conditions. For this purpose, we present a new measurement approach in which only a narrow elastic belt is placed around the thorax to measure the electrical activity of the heart. This belt is equipped with an array of reusable gold-plated dry electrodes. With these dry electrodes, the differential voltages are measured in the horizontal and vertical directions. Afterwards, an approximation of the geometrical potential distribution on the thorax is obtained from these measurements. The results are then visualized as videos or image series or used for further analysis. A subject measurement demonstrates the applicability of this novel approach. It is shown that the obtained Body Surface Potential Maps are very similar to those found in the literature, despite a reduced spatial measurement range. This approach is not only applicable for clinical applications but also suitable for monitoring during physiological training.

I. INTRODUCTION

Electrocardiography (ECG) is one of the most established and best-known electrical biomedical measurement techniques [1]. The aim is to record the activities of the heart by measuring the electrical potentials occurring on the body surface by means of electrodes [2]. The information content of an ECG is related to the number of acquired different channels and therefore depends on the number of contacts with the human body. For maximum information acquisition Body Surface Potential Mapping (BSPM) is used [3]. This technique is based on placing an array of a large number of electrodes on the thorax. Typically, between 64 and several hundred electrodes are applied [3], [4], [5], [6]. This allows not only the analysis of the individual potentials, but also the visualization of the spatial signal propagation. From this, correspondingly more detailed information about the conditions of the heart can be derived. One goal, for instance, is the detection of an ischemic cardiomyopathy [3].

However, the derivation of many electrical potentials is accompanied by technical and practical problems. Precise

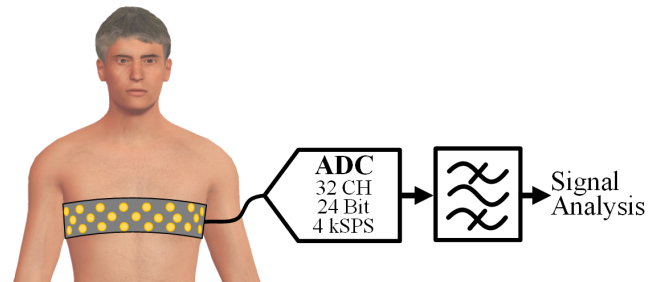


Fig. 1. Measurement setup for body surface potential mapping. The subject wears a dry electrode belt which is electrically connected to a data acquisition system.

placing of the electrodes on the thorax is time-consuming and requires expertise. In addition, the gel electrodes can lead to skin irritation and the removal of adhesive electrodes can be painful [7], [8]. Both the large covered skin surface and the numerous cable connections to the measuring device limit the freedom of patients and clinicians. These problems apply to inpatient and outpatient care. Thus, although the BSPM is technically and medically relevant and useful, it is often too cumbersome for use in the clinical environment.

Therefore, in this manuscript we propose a novel approach that is suitable for everyday use in the clinic. It is based on a reusable dry electrode belt for signal acquisition in combination with a recently published multi-channel signal acquisition system [9].

The 32 differential ECG signals acquired with this setup can be used for several applications. The focus of this work is on the visualization of the spatial electrical potential distribution on the thorax. However, the high redundancy of the signals can also be utilized to calculate a sum signal, which might be useful for robust heart rate monitoring.

II. MATERIALS AND METHODS

A. Measurement Setup

The measurement setup in Figure 1 consists of four interacting components. First, the electrical contacts to the thorax are required. The elastic belt shown in Figure 2 is used for this purpose. It is placed around the thorax and fixed using a velcro fastener. The closure lies on the spine so that the channels are positioned counterclockwise around the thorax. For electrical contacting, the belt is equipped with 49 gold-plated (based on [10]) dry electrodes which are arranged as three staggered rings. The shifts allow the detection of 16 horizontal and 16 vertical differential channels. The gold-

¹Roman Kusche, Andra Oltmann, Jan Graßhoff, and Philipp Rostalski are with Fraunhofer Research Institution for Individualized and Cell-Based Medical Engineering IMTE, 23562 Lübeck, Germany roman.kusche@imte.fraunhofer.de

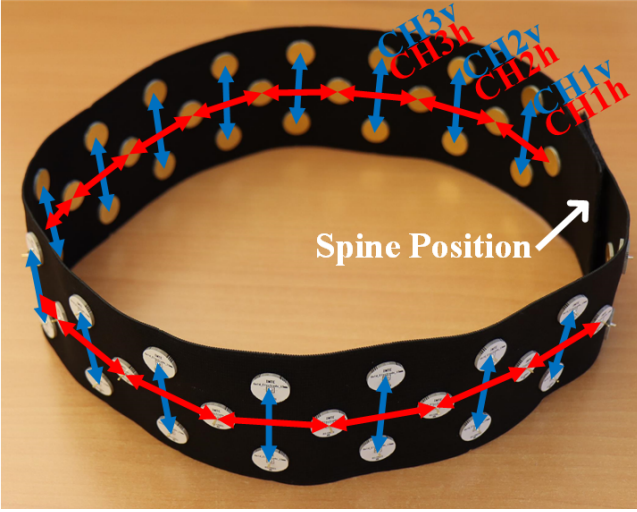


Fig. 2. Stretchable belt equipped with 49 circular gold-plated dry electrodes for differential ECG signal acquisition. The distances between related electrodes are 5 cm in horizontal and vertical direction.

plated electrodes are small round circuit boards connected to the acquisition system via a ribbon cable.

The acquisition system, based on [9], consists of 32 differential ADCs. These digitize the ECG signals with a resolution of 24 bits and a sampling rate of 4kSPS. This significant oversampling of the low-frequency ECG signals results in a beneficial increase of the signal-to-noise ratio. Afterwards, the data is forwarded to a PC for signal processing and analysis. To remove the low-frequency drifts and interferences in frequency ranges above the ECG signals, the acquired signals are digitally high-pass ($N=1$, $f_{c,HP} = 0.5\text{Hz}$) and low-pass ($N=2$, $f_{c,LP} = 10\text{Hz}$) filtered via Matlab (The MathWorks, Natick, MA, US). Although signal components of the ECG are also above 10Hz, their graphical visualization in a BSPM is difficult because of the high temporal resolution required. In the last step, the individual ECG signals are combined to a visualization of the electrical potential propagation.

B. Signal Analysis

The recorded signals can be analyzed in different ways. If the aim is to obtain a robust overall signal, such as for stable heart rate measurement, the information from all channels can be combined. The simplest option here is the accumulation of many different ECG signals. However, it must be considered that signal cancellations can occur due to the different measurement directions.

If a Body Surface Potential Map is to be generated from the acquired information, the individual electrical potentials must first be estimated from the local differential voltages. For a suitable representation, these are mapped into a 3×16 array. Figure 3 shows an example of the first orthogonally arranged electrode pairs of CH1 and CH2 of the belt. V_{1h} , V_{1v} , V_{2h} and V_{2v} represent the differentially measured and digitized voltages.

In the cells of the array in x-direction and y-direction the

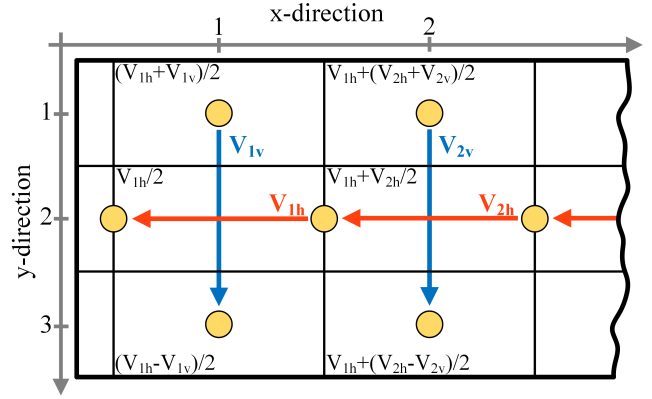


Fig. 3. Illustration of the differential voltages measured between the electrodes (yellow) and the array of approximated electrical potentials for Body Surface Potential Mapping. In each cell the respective formula for the estimated potential is noted.

respective formulas for estimating the potentials $V_{x,y}$ in the center of each cell are noted according to

$$V_{x,1} = \frac{V_{xh}+V_{xv}}{2} + \sum_{k=1}^{x-1} V_{kh}, \quad (1)$$

$$V_{x,2} = \frac{V_{xh}}{2} + \sum_{k=1}^{x-1} V_{kh}, \quad (2)$$

$$V_{x,3} = \frac{V_{xh}-V_{xv}}{2} + \sum_{k=1}^{x-1} V_{kh}. \quad (3)$$

III. RESULTS AND DISCUSSION

A. Signal Acquisition

The presented setup was used to perform first subject measurements which have been approved by the ethics committee of the University of Lübeck (#21-020). For that, the electrode belt was applied to the thorax of a male subject as shown in Figure 1. The velcro fastener was accordingly located over the spine and the channels were arranged counterclockwise on the skin surface. Afterwards, the subject lay down on a treatment table. To ensure good electrical contact, a 5 minute pause was made so that moisture could accumulate between the electrodes and the skin surface. For a duration of 30s, the ECG signals were acquired. The 32 digitized differential signals were filtered and normalized according to section II-A. Figure 4 shows a 5s section of these signals, separated into vertical and horizontal channels.

The typical ECG characteristics, such as the R-wave, are clearly visible. As to be expected, close to the heart (CH8-CH11) the signal amplitudes are particularly high. The influence of the strong band limitation due to the low-pass filtering is visible, but is needed for the graphical representation later in this manuscript.

B. Channel Accumulation

In some applications, the acquisition of a robust ECG is more important than a precise evaluation of the signal shape or spatial signal propagation. These include, for example, heart rate measurements as used in fitness applications.

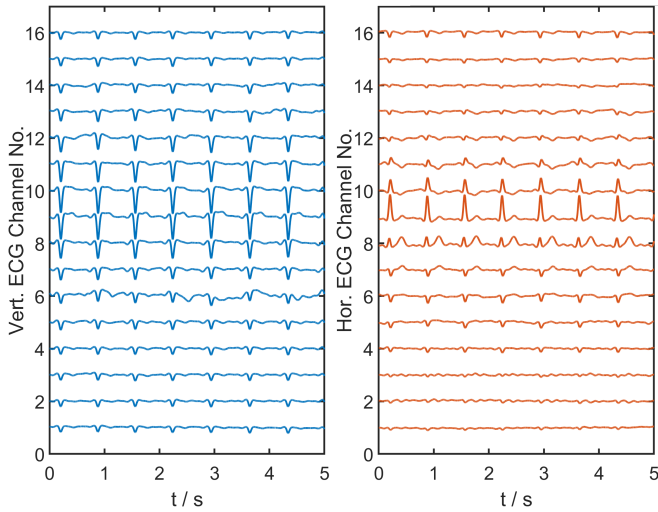


Fig. 4. Digitized and filtered ECG signals of a subject measurement for a duration of 5s. In the left plot the 16 vertically measured differential voltages are shown. In the right plot, the horizontally measured voltages are presented.

For such applications, the high redundancy of the several acquired channels can be combined. To demonstrate this approach, an additional subject measurement was performed under the same conditions as in the section above. In this measurement, the subject has moved, so that the electrode contacts are affected and cause disturbances in some signals. The recorded and filtered 16 vertical EMG signals are plotted in Figure 5.

It can be seen that some of the disturbances that occur are in a similar frequency range to that of ECG signals. A spectral separation therefore does not result in an appropriate interference removal. The accumulated sum signal of these 16 channels is shown at the bottom of Figure 5. Due to the averaging, the influence of the disturbances is significantly reduced and thus, for example, a reliable R-wave detection for the calculation of the heart rate can be achieved. This method is very simple and can of course be significantly improved by more extensive signal processing.

C. Body Surface Potential Mapping

The main purpose of the presented measurement setup is the Body Surface Potential Mapping. For this, the acquired and filtered differential signals are first converted into locally distributed electric potentials according to section II-B. Subsequently, these potentials are visualized as images with 3×16 pixels. The color scale used, ranges from blue (low values) to red (high values) and is limited to the voltage range of the signals. In Figure 6 the resulting images for one heartbeat are shown in time steps of 25ms each. Consistent with the previously used annotations and Figure 3, the left three pixels correspond to the measurement to the right of the spine. The x-direction then corresponds to the counter-clockwise around the thorax worn belt. The x-position 16 thus corresponds to the measurement to the left of the spine. For a temporal orientation, the analyzed ECG signal period is plotted to the left of all images, whereas the red marks

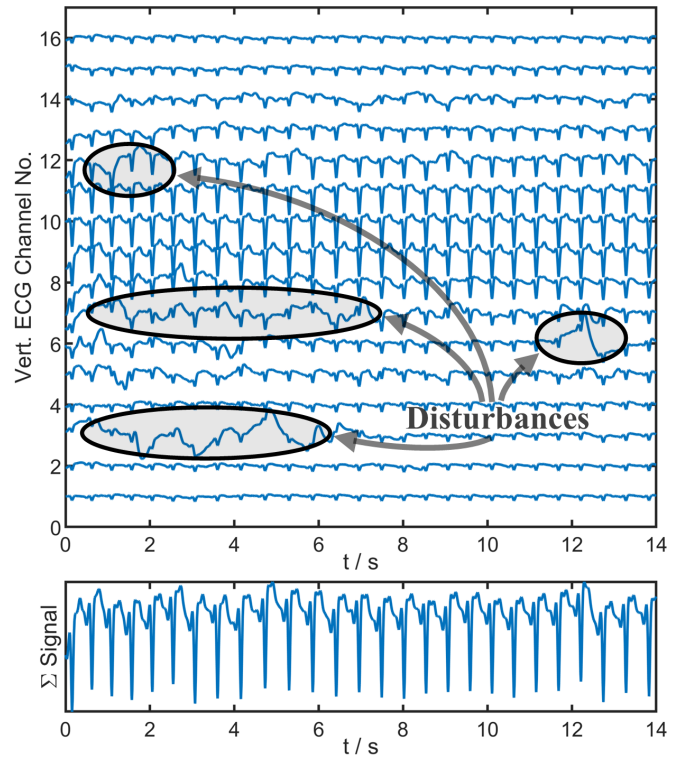


Fig. 5. Measurement results of a study influenced by disturbances. In the lower plot, all 16 vertical ECG channels are accumulated to obtain a robust overall signal.

indicate the corresponding point in time. It is important to note that, in contrast to other works, a common normalization was used for all images [11]. This is an advantage because the constant relationship between colors and voltage values enables a direct comparison of the the individual images.

The time period until approximately $t = 300$ ms includes the PR interval of the ECG. During the corresponding atrial depolarization, it can be observed that the distribution of the electrical potential does almost not change, which is consistent with the literature [11], [12]. During the subsequent QRS complex ($t \approx 325...450$ ms), rapid and strong potential changes occur on the thorax surface, which are difficult to detect with this temporal resolution. This short period of ventricular depolarization is therefore additionally shown in a higher temporal resolution in Figure 7, which will be discussed afterwards. After the ST segment ($t \approx 475...550$ ms), the T wave ($t \approx 575...675$ ms) occurs, which completes this single ECG period. As in the literature, the center of the positive potential is geometrically higher than during the R wave and slightly shifted against the x-direction [11], [12].

The high temporal resolution of 10ms in Figure 7 provides a better visualization of the spatial potential propagation during ventricular depolarization. Thus, the positive potential increase and its shift in x-direction and y-direction during the QR slope can be observed. During the R peak, the typical diagonal potential gradient is clearly visible, which subsequently decreases again.

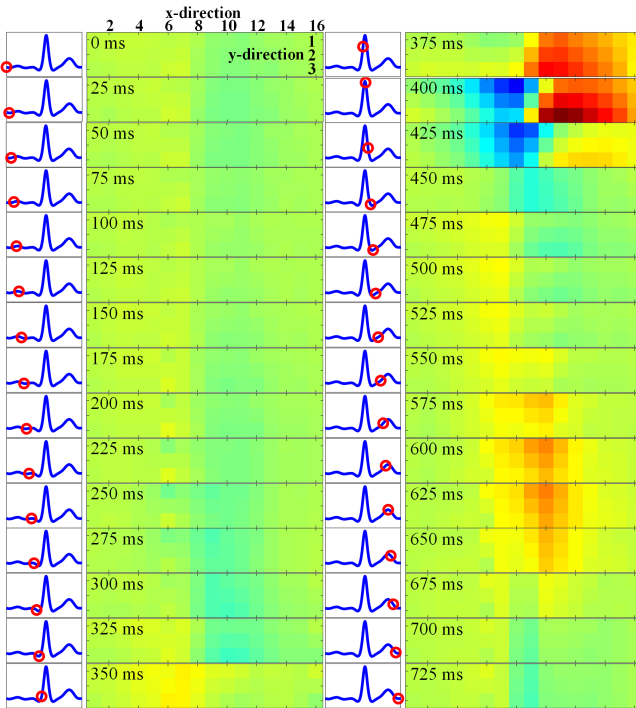


Fig. 6. Visualization of a single ECG period as a Body Surface Potential Map. For better temporal orientation, the corresponding time point is marked in the ECG plot on the left side. The color scale ranges from low potentials (blue) to high potentials (red).

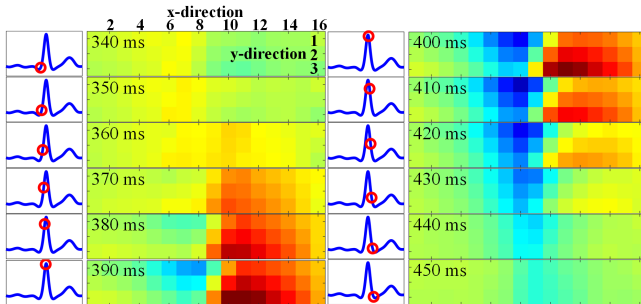


Fig. 7. Body Surface Potential Mapping of the QRS complex with a temporal resolution of 10ms.

IV. CONCLUSION

The goal of this work was to facilitate the use of Body Surface Potential Mapping under realistic conditions. For this purpose, a novel measurement setup for the spatial acquisition of ECG signals was presented, which is especially intended to improve the comfort of patients and medical staff during examination. To achieve unobtrusiveness, a narrow stretchable band was used that covers only a small area of the thorax surface. The signal acquisition is based on the utilization of reusable dry electrodes between which differential voltages are measured in horizontal and vertical direction. The BSPM is then approximated from the digitized information via simple calculations resulting in low required computational efforts.

A first subject study demonstrated the feasibility of this ap-

proach. Despite the narrow belt, the resulting visualizations are comparable to those of conventional BSPM systems. It is conceivable that the vertical limitations of the measuring range are acceptable for certain applications. Especially for fitness or training purposes, in which comfort is of importance, it could be a good compromise. It is also conceivable that the vertical limits of the visualization can be extended via graphical extrapolation [13]. This would not generate any new information but could improve the clarity.

In the future, further studies on subjects and patients would be useful. In order to perform these measurements also under training conditions, the measurement system could be modified. These modifications could include a battery supply and wireless communication interfaces or the possibility to log the measurement data into a portable storage.

ACKNOWLEDGMENT

This work was supported by the European Regional Development Fund, the Federal Government and Land Schleswig-Holstein, Project: “Diagnose- und Therapieverfahren für die Individualisierte Medizintechnik (IMTE)”, Project No. 12420002.

REFERENCES

- [1] M. A. Serhani, H. T. El Kassabi, H. Ismail, and A. Nujum Navaz, “Ecg monitoring systems: Review, architecture, processes, and key challenges,” *Sensors*, vol. 20, no. 6, 2020.
- [2] P. K. Jain and A. K. Tiwari, “Heart monitoring systems—a review,” *Computers in Biology and Medicine*, vol. 54, pp. 1–13, 2014.
- [3] J. Bergquist, L. Rupp, B. Zenger, J. Brundage, A. Busatto, and R. S. MacLeod, “Body surface potential mapping: Contemporary applications and future perspectives,” *Hearts*, vol. 2, no. 4, pp. 514–542, 2021.
- [4] S. Calin, “Spatiotemporal interpolation of body surface potential maps: Methods and errors,” in *10th International Symposium on Electronics and Telecommunications*, 2012, pp. 259–262.
- [5] J. R. Fitz-Clarke, J. L. Sapp, J. W. Warren, J. C. Clements, and B. M. Horacek, “Body surface potential mapping and computer simulation of human ventricular fibrillation,” in *Computers in Cardiology*, 2006, pp. 397–400.
- [6] J. L. Salinet, V. G. Marques, M. Mazzetto, E. D. L. B. Camargo, C. A. Pastore, and I. A. Cestari, “A 64-lead body surface potential mapping system,” in *Computing in Cardiology (CinC)*, 2017, pp. 1–4.
- [7] S. Ramasamy and A. Balan, “Wearable sensors for ecg measurement: a review,” *Sensor Review*, vol. 38, no. 4, pp. 412–419, 2018.
- [8] Y. Fu, J. Zhao, Y. Dong, and X. Wang, “Dry electrodes for human bioelectrical signal monitoring,” *Sensors*, vol. 20, no. 13, 2020.
- [9] R. Kusche, J. Graßhoff, A. Oltmann, L. Boudnik, and P. Rostalski, “A robust multi-channel emg system for lower back and abdominal muscles training,” *Current Directions in Biomedical Engineering*, vol. 7, no. 2, pp. 159–162, 2021.
- [10] R. Kusche, S. Kaufmann, and M. Ryschka, “Dry electrodes for bioimpedance measurements—design, characterization and comparison,” *Biomedical Physics & Engineering Express*, vol. 5, no. 1, p. 015001, 2018.
- [11] Z. Cai, J. Li, K. Luo, X. Zhang, Y. Wang, and J. Zhang, “Design and experimental verification of a recording scheme for body surface potential mapping,” in *Chinese Automation Congress (CAC)*, 2017, pp. 3973–3976.
- [12] M. Medvegy, G. Duray, A. Pintér, and I. Préda, “Body surface potential mapping: Historical background, present possibilities, diagnostic challenges,” *Ann Noninvasive Electrocardiol.*, vol. 7, no. 2, pp. 139–151, 2006.
- [13] J. Graßhoff, A. Jankowski, and P. Rostalski, “Scalable Gaussian process separation for kernels with a non-stationary phase,” in *Proceedings of the 37th International Conference on Machine Learning. PMLR*, 13–18 Jul 2020, pp. 3722–3731.